International Journal of Control, Automation and Systems 15(6) (2017) 2704-2713
http://dx.doi.org/10.1007/s12555-016-0562-0
ISSN:1598-6446 eISSN:2005-4092
http://www.springer.com/12555

Formation Tracking Control for Multi-agent Systems: A Wave-equation based Approach

Shu-Xia Tang, Jie Qi*, and Jing Zhang

Abstract: This paper considers the formation tracking control problem of large-scaled Multi-Agent Systems (MAS) for which the model is based on a system of mutually independent wave Partial Differential Equations (PDEs). The spatial derivatives in the equation correspond to the underlying communication topology of the agents. A leader-follower mode is employed in the control algorithm, with which the agents on the boundary of PDEs are chosen as leaders knowing the tracking trajectory and all the other agents are followers. Each follower has only the information of its own relative position and velocity to its topological neighbors. With a designed distributed controller, the formation tracking error is bounded by a constant proportional to the acceleration of the desired trajectory. Robustness of the control law to a perturbation in the velocity measurement is also discussed. Furthermore, some simulation studies are provided to show the effectiveness of the control algorithm.

Keywords: Distributed control, formation tracking, MAS, robustness, wave PDE.

1. INTRODUCTION

Compared with static deployment, dynamic formation tracking control is more challenging and has more applications. Formation tracking control have wide applications in formation flight, air traffic control, exploration, navigation in a group, cooperative carrying and coordinated path following, etc [1–3]. The problem of formation tracking, or coordinated tracking, is often formulated as determining a coordinated control law that keeps the multi-agent systems maintain a desired, possibly time-varying, formation while tracking a target or following a reference orbit.

In most of the existing literatures, formation control for MAS is modeled by a system of Ordinary Differential Equations (ODEs), in which each agent corresponds to an ODE [4, 5]. While the number of the agents increases, the system modeled by ODEs becomes more complex and thus can be more difficult to analyze the macro-dynamics. Recently, the coordinate control of multi-agent system with thousands of agents has attracted great attention [6, 7]. Inspired by the application of Lagrangian spatial coordinates in the modeling of large-scale collective hydrodynamics [8], large-scale MAS can be modelled by PDEs by treating all the agents as a continuum [9].

The PDE-based approach is more suitable than the ODE-based method in control design and analyzing large-scale systems. Besides, it can generate more diversified and more interesting desirable formation manifolds in a 2-D and even higher dimensional spaces. The Laplace consensus laws can then be approximated by the corresponding discretized version of the Laplace operators in the PDEs [10]. In fact, the PDE-based approach has been successfully applied into agent deployment [11–13], coordinated searching [14], vehicular platoons [15], distributed detecting pipeline leakage [16], opinion dynamics [17] and configuration transitions with collision and obstacle avoiding [18]. When employing the PDE-based approach, There are several main contributions in the paper.

- A second-order wave PDE model is proposed with actuation on the accelerations of the agents, while most researchers choose the parabolic PDE which describes the first-order dynamics. Indeed, since the inputs actuated on the agents are usually forces or torques, acceleration control has wider applications [19, 20] than velocity control. Furthermore, when the acceleration of the desired trajectories is equal to zero, the proposed distributed control actuating on the acceleration makes the formation tracking error con-

Manuscript received September 9, 2016; revised March 16, 2017; accepted April 30, 2017. Recommended by Associate Editor Hyo-Sung Ahn under the direction of Editor Duk-Sun Shim. This work was partially supported by National Natural Science Foundation of China 61773112, 61473265, Natural Science Foundation of Shanghai 16ZR1401200 and the Fundamental Research Funds for the Central Universities 2232015D3-24.

Shu-Xia Tang is with the Department of Mechanical & Aerospace Engineering, University of California, San Diego, La Jolla, CA 92093, USA (e-mail: sht015@ucsd.edu). Jie Qi is with the College of Information Science and Technology and Engineering Research Center of Digitized Textile and Fashion Technology, Ministry of Education, Donghua University, Shanghai 201620, China (e-mail: jieqi@dhu.edu.cn). Jing Zhang is with the College of Information Science and Technology, Donghua University, Shanghai 201620, China (e-mail: zhangj0811@163.com).
* Corresponding author.

verges to zero. While our previous work [21] with the control actuating on the velocity has tracking error in the same situation of zero acceleration.

- In the literature of formation tracking control, e.g., [1, 22], the reference orbit is the global information for all agents. But for the system with thousands of agents, it is energy-consuming to inform each agent where the target is. We loose this constraint by assuming that only a few of agents i.e., the leaders chosen as the agents on boundary of the PDEs know the desired trajectory. The other agents are followers. All the information that is needed for control of a follower is an agent's relative position and relative velocity to its neighbors, so this method is suitable for applications in room where the Global Positioning System (GPS) signal is weak and not accurate.
- The wave PDE is not convergent due to the energy conservation. In the paper, we introduce a Kelvin-Voigt damping term which allows the PDE model to converge. The added damping term is applied to actuate the acceleration with the velocity feedback such that tracking errors are bounded by a constant proportional to the acceleration of the desired trajectory. Robustness of the control law to a perturbation in the velocity measurement is analyzed, and a range of the velocity inaccuracy is given within which the controller remains effective, i.e., to guarantee that tracking error converges to a bounded region or converges to zero due to a zero acceleration of the desired trajectory.

The remaining parts of this paper is organized as follows. Section 2 models the large-scale MAS by a wave PDE and states the formation tracking control problem. Introducing a Kelvin-Voigt damping into the distributed controller for the PDE system, the formation tracking errors under a leader-follower strategy are proved to be bounded in Section 3. Section 4 studies robustness of the control law to a perturbation in the velocity measurement. Section 5 presents several numerical simulations for 3-D formation tracking with 2-D spherical surface topology, illustrating that the proposed control algorithm in this paper is effective for the formation tracking control of MAS. Finally, some concluding remarks are presented in Section 6.

2. PROBLEM STATEMENT

2.1. Multi-agent PDE system

Consider an MAS under the following consensus control protocol [5]:

$$\ddot{\mathbf{w}}_{\mathbf{k}} = \sum_{\mathbf{j}\in\mathcal{N}_k} a_{\mathbf{k},\mathbf{j}} \left(\mathbf{w}_{\mathbf{j}} - \mathbf{w}_{\mathbf{k}}\right), \tag{1}$$

where $\mathbf{w}_k \in D \subset \mathbb{R}^n$ denotes the position for the agent labeled by $\mathbf{k} \in I \subset (\mathbb{N}^*)^m$, with I denoting the (discrete) set of the agent label and m denoting the dimension of the corresponding topology. Moreover, $\mathcal{N}_k \subset I$ is the set of neighbors of the agent $\mathbf{k}$, and $a_{\mathbf{k},\mathbf{j}} \in \mathbb{R}_{\geq 0}$ is the linkage weight between the agents $\mathbf{k}$ and $\mathbf{j}$. Implied by the second-order time derivative on the left hand side, the control protocol is applied onto the acceleration of the agents.

Treating the large-scale MAS as a continuum, i.e., mapping the discrete agent label set I into a continuous space $\Omega \subset \mathbb{R}^m$, each agent can then be labeled by a vector $\boldsymbol{\alpha} = (\alpha_1, \alpha_2, \cdots \alpha_m) \in \Omega$, which gives the topology location of the agent in the continuous communication topology Ω. Assume that the topology domain Ω is bounded with a C^∞ boundary $\partial\Omega$. For each agent $\boldsymbol{\alpha}$, let the vector

$$\mathbf{w}(\boldsymbol{\alpha},t) = (w^1(\boldsymbol{\alpha},t), w^2(\boldsymbol{\alpha},t), \cdots, w^n(\boldsymbol{\alpha},t))^T \subset \mathbb{R}^n$$

represent its real-time position in an n-dimensional state space, with each element $w^i(\boldsymbol{\alpha},t), i \in \{1,2,\cdots,n\}$ denoting the coordinate in the i-th dimension.

Noticing that the consensus control protocol on the right hand side of (1) is the discretized version of the Laplace operator [23], the system of ODEs (1) is then written into a wave PDE:

$$\mathbf{w}_{tt}(\boldsymbol{\alpha},t) = k_1 \Delta \mathbf{w}(\boldsymbol{\alpha},t),$$

where $k_1 > 0$, $\mathbf{w}_{tt}(\boldsymbol{\alpha},t)$ denotes the acceleration of the agent $\boldsymbol{\alpha} \in \Omega$, and Δ denotes the Laplace operator.

2.2. Formation tracking control problem

This paper is mainly concerned about the formation tracking problem, i.e., to make sure that all the agents as a whole, while keeping some pre-designated formation, track some pre-designated trajectory. Denote the desired formation as

$$\mathbf{w}^d(\boldsymbol{\alpha}) = (w^{1,d}(\boldsymbol{\alpha}), w^{2,d}(\boldsymbol{\alpha}), \cdots, w^{n,d}(\boldsymbol{\alpha}))^T \in H^m(\Omega, \mathbb{R}^n),$$

and denote the trajectory which the agents would track uniformly as

$$\mathbf{f}(t) = (f_1(t), f_2(t), \cdots, f_n(t))^T \in C^3(\mathbb{R}_{\geq 0}, \mathbb{R}^n).$$

Given that the MAS is linear, the aimed moving formation that the agents would track as a whole can be formulated as a simple superposition of the desired formation and trajectory:

$$\mathbf{w}^r(\boldsymbol{\alpha},t) = \mathbf{w}^d(\boldsymbol{\alpha}) + \mathbf{f}(t). \tag{2}$$

The leader-follower strategy is employed. More precisely, we choose the agents on boundary $\partial\Omega$ as leaders, which have the information of both their desired (relative) positions $\mathbf{w}^d(\boldsymbol{\alpha})|_{\boldsymbol{\alpha}=\partial\Omega}$ in the formation and the desired positions in the trajectory $\mathbf{f}(t)$. In other words, the boundary agents $\boldsymbol{\alpha} \in \partial\Omega$ follow the moving formation

$\mathbf{w}^r(\boldsymbol{\alpha},t)|_{\boldsymbol{\alpha}\in\partial\Omega}$, which gives the following boundary condition for the MAS:

$$\mathbf{w}(\boldsymbol{\alpha},\mathbf{t})|_{\boldsymbol{\alpha}\in\partial\Omega}=\mathbf{w}^r(\boldsymbol{\alpha},t)|_{\boldsymbol{\alpha}\in\partial\Omega}=\mathbf{w}^d|_{\boldsymbol{\alpha}\in\partial\Omega}+\mathbf{f}(t). \tag{3}$$

On the other hand, all the other agents are treated as followers, which only know their own relative positions to the topology neighbors. In order for all the agents (including the followers) to achieve the desired formation tracking, we would like to seek a distributed feedback controller $\mathbf{u}(\boldsymbol{\alpha},t)$ such that the state of the resultant controlled PDE

$$\mathbf{w}_{tt}(\boldsymbol{\alpha},t)=k_1\Delta\mathbf{w}(\boldsymbol{\alpha},t)+\mathbf{u}(\boldsymbol{\alpha},t) \tag{4}$$

tracks $\mathbf{w}^r(\boldsymbol{\alpha},t)$. The initial condition is denoted as

$$\mathbf{w}(\boldsymbol{\alpha},0)=\mathbf{w}_0(\boldsymbol{\alpha}),\quad \mathbf{w}_t(\boldsymbol{\alpha},0)=\mathbf{w}_1(\boldsymbol{\alpha}). \tag{5}$$

3. FORMATION TRACKING CONTROL

3.1. Formation tracking control design

Introduce the tracking error $\tilde{\mathbf{w}}=\mathbf{w}-\mathbf{w}^r$, then it immediately follows from (4) and (2) that the error dynamics is governed by

$$\tilde{\mathbf{w}}_{tt}(\boldsymbol{\alpha},t)=k_1\Delta\mathbf{w}(\boldsymbol{\alpha},t)+\mathbf{u}(\boldsymbol{\alpha},t)-\mathbf{f}''(t). \tag{6}$$

If choosing the inner controller as

$$\mathbf{u}(\boldsymbol{\alpha},t)=-k_1\Delta\mathbf{w}^d(\boldsymbol{\alpha}),$$

then the error system becomes

$$\begin{aligned}&\tilde{\mathbf{w}}_{tt}(\boldsymbol{\alpha},t)=k_1\Delta\tilde{\mathbf{w}}(\boldsymbol{\alpha},t)-\mathbf{f}''(t),\\&\tilde{\mathbf{w}}(\boldsymbol{\alpha},t)|_{\boldsymbol{\alpha}\in\partial\Omega}=0,\\&\tilde{\mathbf{w}}(\boldsymbol{\alpha},0)=\tilde{\mathbf{w}}_0(\boldsymbol{\alpha}),\quad \tilde{\mathbf{w}}_t(\boldsymbol{\alpha},0)=\tilde{\mathbf{w}}_1(\boldsymbol{\alpha}).\end{aligned}$$

It is well known that for the case of $\mathbf{f}''(t)=\mathbf{0},\forall t\in(0,\infty)$, the above system is energy conservative, which further implies that the agents cannot track the desired formation $\mathbf{w}^r(\boldsymbol{\alpha},t)$ even when $\mathbf{f}''(t)=\mathbf{0}$.

Consider instead the following distributed controller:

$$\mathbf{u}(\boldsymbol{\alpha},t)=-k_1\Delta\mathbf{w}^d(\boldsymbol{\alpha})+k_2\Delta\mathbf{w}_t(\boldsymbol{\alpha},t), \tag{7}$$

by which a Kelvin-Voigt damping [24, Chapter 7] with the weight $k_2>0$ is incorporated into the resultant controlled system. $\mathbf{w}_t(\boldsymbol{\alpha},t)$ denotes the velocity of the agent $\boldsymbol{\alpha}\in\Omega$, and the operator Δ further denotes the information (i.e., position or velocity) exchange among the agent with its neighbors. From (2), (3), (6) and (7), the resultant tracking error system is

$$\begin{aligned}&\tilde{\mathbf{w}}_{tt}(\boldsymbol{\alpha},t)=k_1\Delta\tilde{\mathbf{w}}(\boldsymbol{\alpha},t)+k_2\Delta\tilde{\mathbf{w}}_t(\boldsymbol{\alpha},t)-\mathbf{f}''(t),\\&\tilde{\mathbf{w}}(\boldsymbol{\alpha},t)|_{\boldsymbol{\alpha}\in\partial\Omega}=0,\\&\tilde{\mathbf{w}}(\boldsymbol{\alpha},0)=\tilde{\mathbf{w}}_0(\boldsymbol{\alpha}),\quad \tilde{\mathbf{w}}_t(\boldsymbol{\alpha},0)=\tilde{\mathbf{w}}_1(\boldsymbol{\alpha}),\end{aligned}$$

where it follows from (5) that

$$\tilde{\mathbf{w}}_0(\boldsymbol{\alpha})=\mathbf{w}_0(\boldsymbol{\alpha})-\mathbf{w}^r(\boldsymbol{\alpha},0),\tilde{\mathbf{w}}_1(\boldsymbol{\alpha})=\mathbf{w}_1(\boldsymbol{\alpha})-\mathbf{f}'(0).$$

3.2. Stability of the formation tracking error system

Note that the equation for each coordinate $i=1,\cdots,n$ is of the same type and is independent from each other, we consider only the dynamics of $\tilde{w}_1(\boldsymbol{\alpha},t)$ in the sequel, keeping in mind that the same result holds for the dynamics of the other coordinates as well. For the denotation convenience, we write $\tilde{w}_1,f_1$ by $\tilde{w},f$. Therefore, the tracking error system in consideration is rewritten as

$$\tilde{w}_{tt}(\boldsymbol{\alpha},t)=k_1\Delta\tilde{w}(\boldsymbol{\alpha},t)+k_2\Delta\tilde{w}_t(\boldsymbol{\alpha},t)-f''(t), \tag{8}$$

$$\tilde{w}(\boldsymbol{\alpha},t)|_{\boldsymbol{\alpha}\in\partial\Omega}=0, \tag{9}$$

$$\tilde{w}(\boldsymbol{\alpha},0)=\tilde{w}_0(\boldsymbol{\alpha}),\quad \tilde{w}_t(\boldsymbol{\alpha},0)=\tilde{w}_1(\boldsymbol{\alpha}). \tag{10}$$

Define the space

$$H^k=\{x\in L^2(\Omega)|\ \bigtriangledown^p x(\boldsymbol{\alpha},t)\in L^2(\Omega)\ \text{ for }\ |p|\le k\},$$

with the norm

$$\|x\|_{H^k}=\left(\sum_{|p|\le k}\int_\Omega|\bigtriangledown^p x|^2\right)^{\frac{1}{2}},$$

and let the space

$$H_0^1=\{x\in H^1(\Omega)|\ x=0\ \text{ on }\ \partial\Omega\},$$

then the following theorem can be derived.

Theorem 1: Suppose the acceleration of the moving formation is bounded by as constant γ, i.e., $|f''(t)|\le\gamma$, $\forall t\ge0$, then for any initial condition

$$(\tilde{w}_0,\ \tilde{w}_1)\in(H^m(\Omega)\cap H_0^1(\Omega))^2$$

satisfying the compatibility condition

$$\tilde{w}_0(\boldsymbol{\alpha},0)|_{\boldsymbol{\alpha}=\partial\Omega}=0,\qquad \tilde{w}_1(\boldsymbol{\alpha},0)|_{\boldsymbol{\alpha}=\partial\Omega}=0, \tag{11}$$

there exists a unique solution

$$\tilde{w}(\cdot,t)\in C([0,\infty);H^1(\Omega))\cap C^1([0,\infty);L^2(\Omega))$$

to the error system (8) – (10). Moreover, there exist positive constants ω, C_1 and C_2, such that

$$\|\tilde{w}(\cdot,t)\|_1\le C_1+e^{-\omega_1 t}\left(C_2\|\tilde{w}(\cdot,0)\|_1-C_1\right), \tag{12}$$

where the norm $\|\cdot\|_1:=\|\cdot\|_{H^1}+\|\cdot_t\|_{L^2}$.

Proof: Well-posedness of the error system (8) – (10) can be referred to [25, Theorem 2.3].

Define a Lyapunov function candidate as

$$\begin{aligned}V(t)=&\frac{1}{2}\int_\Omega\left(\tilde{w}_t(\boldsymbol{\alpha},t)^2+(k_1+ck_2)|\bigtriangledown\tilde{w}(\boldsymbol{\alpha},t)|^2\right)d\boldsymbol{\alpha}\\&+c\int_\Omega\tilde{w}_t(\boldsymbol{\alpha},t)\tilde{w}(\boldsymbol{\alpha},t)d\boldsymbol{\alpha},\end{aligned} \tag{13}$$

where the constant $c>0$ is to be determined later.

Postive definiteness of $V(t)$**.** By the use of Young's Inequality, we have

$$\int_\Omega \tilde{w}_t(\boldsymbol{\alpha},t)\tilde{w}(\boldsymbol{\alpha},t)d\boldsymbol{\alpha} \le \frac{1}{2}\int_\Omega \tilde{w}_t(\boldsymbol{\alpha},t)^2 d\boldsymbol{\alpha} + \frac{1}{2}\int_\Omega \tilde{w}(\boldsymbol{\alpha},t)^2 d\boldsymbol{\alpha}.$$

Moreover, from the Friedrichs' inequality

$$\int_\Omega z(\boldsymbol{\alpha},t)^2 d\boldsymbol{\alpha} \le C\int_\Omega |\bigtriangledown z(\boldsymbol{\alpha},t)|^2 d\boldsymbol{\alpha} \quad \text{for } z|_{\partial\Omega}=0, \quad (14)$$

where the positive constant C depends on the dimensional number n and the domain Ω, it can be obtained that

$$\begin{aligned}&\left(\rho_2-\frac{c}{2}\right)\int_\Omega \tilde{w}_t^2 d\boldsymbol{\alpha} + \left(\rho_2-\frac{cC}{2}\right)\int_\Omega |\bigtriangledown \tilde{w}|^2 d\boldsymbol{\alpha}\\ &\le V(t)\\ &\le (\rho_1+\frac{c}{2})\int_\Omega \tilde{w}_t^2 d\boldsymbol{\alpha} + \left(\rho_1+\frac{cC}{2}\right)\int_\Omega |\bigtriangledown \tilde{w}|^2 d\boldsymbol{\alpha},\end{aligned} \quad (15)$$

where

$$\rho_1 = \frac{1}{2}\max\{1, k_1+ck_2\},\ \ \rho_2 = \frac{1}{2}\min\{1, k_1+ck_2\}. \quad (16)$$

Without loss of generality, assume that $C \ge 1$. Then, by choosing the positive constant c to satisfy

$$0 < c < \min\left\{\frac{1}{C}, \frac{k_1}{|C-k_2|}\right\}, \quad (17)$$

it immediately follows from (15) that

$$0 < c < 2\rho_2 \min\left\{1,\ \frac{1}{C}\right\}, \quad (18)$$

and thus the positive definiteness of $V(t)$ is guaranteed.

Moreover, it can be obtained from (15) that

$$m_1\|\tilde{w}\|_2^2 \le V \le m_2\|\tilde{w}\|_2^2, \quad (19)$$

where the norm

$$\|\cdot\|_2 := \|\bigtriangledown\cdot\|_{L^2} + \|\cdot_t\|_{L^2},$$

and the constants

$$m_1 = \frac{1}{2}\left(\rho_2 - \frac{cC}{2}\right),\ \ m_2 = \rho_1 + \frac{cC}{2}. \quad (20)$$

Calculation of $\dot{V}(t)$**.** Taking the time derivative of $V(t)$ along the trajectory of the error system (8) – (10), we have

$$\begin{aligned}\dot{V} &= \int_\Omega \tilde{w}_t\tilde{w}_{tt}d\boldsymbol{\alpha} + (k_1+ck_2)\int_\Omega \bigtriangledown\tilde{w}_t\cdot\bigtriangledown\tilde{w}d\boldsymbol{\alpha}\\ &\quad + c\int_\Omega(\tilde{w}_{tt}\tilde{w}+|\tilde{w}_t|^2)d\boldsymbol{\alpha}\\ &= -k_2\int_\Omega|\bigtriangledown\tilde{w}_t|^2 d\boldsymbol{\alpha} - ck_1\int_\Omega|\bigtriangledown\tilde{w}|^2 d\boldsymbol{\alpha}\\ &\quad + c\int_\Omega \tilde{w}_t^2 d\boldsymbol{\alpha} - f''\int_\Omega(\tilde{w}_t+c\tilde{w})d\boldsymbol{\alpha},\end{aligned} \quad (21)$$

where the Green's formula

$$\int_\Omega \bigtriangledown u\cdot\bigtriangledown v dx = -\int_\Omega u\Delta v dx + \int_{\partial\Omega}\frac{\partial v}{\partial\nu}u dS$$

is used. Here, ν is the outward-pointing unit normal vector of $\partial\Omega$, and dS denotes the integration element on $\partial\Omega$. From the Friedrichs' inequality (14), we have

$$\begin{aligned}\dot{V} \le &-\left(\frac{k_2}{C}-c\right)\|\tilde{w}_t\|_{L^2}^2 - ck_1\|\bigtriangledown\tilde{w}\|_{L^2}^2\\ &+|f''|(\|\tilde{w}_t\|_{L^2}+c\sqrt{C}\|\bigtriangledown\tilde{w}\|_{L^2}).\end{aligned}$$

Choose the positive parameter c to satisfy $k_2/C - c > 0$, which, together with (17), gives the bound for c as

$$0 < c < \min\left\{\frac{1}{C}, \frac{k_1}{|C-k_2|}, \frac{k_2}{C}\right\}. \quad (22)$$

Let

$$a_1 = \min\left\{\frac{k_2}{C}-c, ck_1\right\},\quad b = \max\{1, c\sqrt{C}\}, \quad (23)$$

then

$$\dot{V} \le -\frac{a_1}{2}\|\tilde{w}\|_2^2 + |f''|b\|\tilde{w}\|_2 \le -\frac{a_1}{2m_2}V + \frac{b}{\sqrt{m_1}}\gamma\sqrt{V},$$

where the inequality (19) is used. Let $W=\sqrt{V}$, then $\dot{W} = \dot{V}/(2\sqrt{V})$, which leads to

$$\dot{W} \le -\frac{a_1}{4m_2}W + \frac{b\gamma}{2\sqrt{m_1}}, \quad (24)$$

and thus the comparison principle for ODE gives

$$\begin{aligned}W(t) &\le \exp\left(-\frac{a_1}{4m_2}t\right)W(0)\\ &\quad + \frac{4b\gamma m_2}{2a_1\sqrt{m_1}}\left(1-\exp\left(-\frac{a_1}{4m_2}t\right)\right)\\ &= \frac{4b\gamma m_2}{2a_1\sqrt{m_1}}\\ &\quad + \exp\left(-\frac{a_1}{4m_2}t\right)\left(W(0)-\frac{4b\gamma m_2}{2a_1\sqrt{m_1}}\right).\end{aligned} \quad (25)$$

From the Friedrichs' inequality (14), there exist positive constants m_3 and m_4 such that

$$m_3\|\tilde{w}\|_2^2 \le \|\tilde{w}\|_1^2 \le m_4\|\tilde{w}\|_2^2, \quad (26)$$

where

$$m_3 = 1,\ m_4 = 1+C. \quad (27)$$

The inequalities (19) and (26) then further gives

$$\frac{m_3}{m_2}V \le \|\tilde{w}\|_1^2 \le \frac{m_4}{m_1}V. \tag{28}$$

From the inequalities (19) and (28), we obtain (12), where

$$C_1 = \frac{4b\gamma m_2}{2a_1 m_1}\sqrt{m_4},\ \ \omega_1 = \frac{a_1}{4m_2},\ \ C_2 = \sqrt{\frac{m_2 m_4}{m_1 m_3}}. \tag{29}$$

Here, a_1, b are defined in (23) with c chosen based on (22). The proof is thus completed. □

From Theorem 1, the formation tracking error resulted from the designed control law (7) is uniformly ultimately bounded by a constant directly proportional to the acceleration of the desired trajectory. Furthermore, if the desired formation is moving with a constant velocity, then under the controller (7), the formation tracking error system is exponentially convergent, which is stated in the following corollary.

Corollary 1: Suppose the acceleration of the moving formation $|f''| = 0$, $\forall t \ge 0$, then for any initial condition $(\tilde{w}_0,\ \tilde{w}_1) \in (H^m(\Omega)\cap H_0^1(\Omega))^2$ satisfying the compatibility condition (11), the unique solution $\tilde{w}(\cdot,t)$ to the error system (8) – (10) is exponentially convergent:

$$\|\tilde{w}(\cdot,t)\|_1 \le C_2 e^{-\omega_1 t}\|\tilde{w}(\cdot,0)\|_1,$$

where C_2, ω_1 are defined in (29), with m_1, m_2, m_3, m_4 defined by (20), (27) and (16), (22).

In other words, the formation tracking error is eliminated exponentially in the case that all the agents moves in a constant velocity. This is an advantage of applying the control law onto the acceleration of the agents over applying the controller onto their velocity [21].

4. ROBUSTNESS TO THE UNCERTAINTY IN THE VELOCITY FEEDBACK

It is thus important to study robustness of the controlled formation tracking system to a small perturbation in the velocity feedback, i.e., the system (4) under the controller

$$\mathbf{u}(\boldsymbol{\alpha},t) = -k_1\Delta\mathbf{w}^d(\boldsymbol{\alpha}) + k_2(1+\varepsilon)\Delta\mathbf{w}_t(\boldsymbol{\alpha},t),$$

where the parameter ε denotes a maximal possible uncertainty of the velocity, which is allowed to be either positive or negative. Without loss of generality, we assume $|\varepsilon| < 1$.

In this case, consider the dynamics of the resultant closed-loop multi-agent system as follows:

$$\begin{aligned}\mathbf{w}_{tt}(\boldsymbol{\alpha},t) &= k_1(\Delta\mathbf{w}(\boldsymbol{\alpha},t) - \Delta\mathbf{w}^d(\boldsymbol{\alpha})) \\ &\quad + k_2(1+\varepsilon)\Delta\mathbf{w}_t(\boldsymbol{\alpha},t), \end{aligned}\tag{30}$$

$$\mathbf{w}(\boldsymbol{\alpha},t)|_{\boldsymbol{\alpha}\in\partial\Omega} = \mathbf{w}^d(\boldsymbol{\alpha},t)|_{\boldsymbol{\alpha}\in\partial\Omega} + \mathbf{f}(t), \tag{31}$$

$$\mathbf{w}(\boldsymbol{\alpha},0) = \mathbf{w}_0(\boldsymbol{\alpha}),\quad \mathbf{w}_t(\boldsymbol{\alpha},0) = \mathbf{w}_1(\boldsymbol{\alpha}), \tag{32}$$

Then the error system becomes

Then,we examine the new $\tilde{\mathbf{w}}_1 = \tilde{w}$-error (scalar) system:

$$\tilde{w}_{tt}(\boldsymbol{\alpha},t) = k_1\Delta\tilde{w}(\boldsymbol{\alpha},t) + k_2(1+\varepsilon)\Delta\tilde{w}_t(\boldsymbol{\alpha},t) - f''(t), \tag{33}$$

$$\tilde{w}(\boldsymbol{\alpha},t)|_{\boldsymbol{\alpha}\in\partial\Omega} = 0, \tag{34}$$

$$\tilde{w}(\boldsymbol{\alpha},0) = \tilde{w}^0(\boldsymbol{\alpha}),\quad \tilde{w}_t(\boldsymbol{\alpha},0) = \tilde{w}^1(\boldsymbol{\alpha}) \tag{35}$$

Theorem 2: Suppose there exists a constant γ such that $|f''(t)| \le \gamma$, $\forall t \ge 0$, then there exists a constant $\varepsilon^* > 0$ such that for any positive constant ε satisfying $|\varepsilon| < \varepsilon^*$, for any initial condition $(\tilde{w}^0,\ \tilde{w}^1) \in (H^m(\Omega)\cap H_0^1(\Omega))^2$ satisfying the compatibility boundary conditions

$$\tilde{w}^0(\boldsymbol{\alpha})|_{\boldsymbol{\alpha}\in\partial\Omega} = 0,\ \tilde{w}^1(\boldsymbol{\alpha})|_{\boldsymbol{\alpha}\in\partial\Omega} = 0,$$

the new error system (33) – (35) admits a unique solution $\tilde{w}(\cdot,t) \in C([0,\infty);H^1(\Omega))\cap C^1([0,\infty);L^2(\Omega))$. Moreover, there exist positive constants ω_2 and C_3 such that

$$\|\tilde{w}(\cdot,t)\|_1 \le C_3 + e^{-\omega_2 t}\left(C_2\|\tilde{w}(\cdot,0)\|_1 - C_3\right), \tag{36}$$

where the norm $\|\cdot\|_1 := \|\cdot\|_{H^1} + \|\cdot_t\|_{L^2}$.

Proof: Calculating the time derivative of the Lyapunov function $V(t)$, defined in (13) with c satisfying (22), along the trajectory of the new error system (33) – (35), we have

$$\begin{aligned}\dot{V}(t) &= -k_2(1+\varepsilon)\int_\Omega |\bigtriangledown\tilde{w}_t|^2 d\boldsymbol{\alpha} + ck_2\varepsilon\int_\Omega \tilde{w}_t\Delta\tilde{w}\,d\boldsymbol{\alpha} \\ &\quad - ck_1\int_\Omega |\bigtriangledown\tilde{w}|^2 d\boldsymbol{\alpha} + c\int_\Omega \tilde{w}_t^2 d\boldsymbol{\alpha} \\ &\quad - f''\int_\Omega (\tilde{w}_t + c\tilde{w})d\boldsymbol{\alpha} \\ &= -k_2(1+\varepsilon)\int_\Omega |\bigtriangledown\tilde{w}_t|^2 d\boldsymbol{\alpha} \\ &\quad - ck_2\varepsilon\int_\Omega \bigtriangledown\tilde{w}_t\bigtriangledown\tilde{w}\,d\boldsymbol{\alpha} \\ &\quad - ck_1\int_\Omega |\bigtriangledown\tilde{w}|^2 d\boldsymbol{\alpha} + c\int_\Omega \tilde{w}_t^2 d\boldsymbol{\alpha} \\ &\quad - f''\int_\Omega (\tilde{w}_t + c\tilde{w})d\boldsymbol{\alpha} \\ &\le -\frac{1}{2}k_2\left(2(1+\varepsilon) - c|\varepsilon|\right)\int_\Omega |\bigtriangledown\tilde{w}_t|^2 d\boldsymbol{\alpha} \\ &\quad - c(k_1 - \frac{1}{2}k_2|\varepsilon|)\int_\Omega |\bigtriangledown\tilde{w}|^2 d\boldsymbol{\alpha} \\ &\quad + c\int_\Omega \tilde{w}_t^2 d\boldsymbol{\alpha} - f''\int_\Omega (\tilde{w}_t + c\tilde{w})d\boldsymbol{\alpha}, \end{aligned}$$

where integration by parts is used in the second equality, the Cauchy-Schwarz inequality and the Young's inequality are used in the inequality. then

$$\begin{aligned}\dot{V}(t) &\le -\left(k_2\frac{2(1+\varepsilon) - c|\varepsilon|}{2C} - c\right)\int_\Omega \tilde{w}_t^2 d\boldsymbol{\alpha} \\ &\quad - c(k_1 - \frac{1}{2}k_2|\varepsilon|)\int_\Omega |\bigtriangledown\tilde{w}|^2 d\boldsymbol{\alpha} \end{aligned}$$

$$
\begin{aligned}
&+\gamma\left(\|\tilde{w}_t\|_{L^2}+c\sqrt{C}\|\bigtriangledown\tilde{w}\|_{L^2}\right)\\
=&-\left(\frac{k_2}{C}-c-\frac{k_2}{C}\left(1-\frac{c}{2}\right)|\varepsilon|\right)\int_\Omega|\tilde{w}_t|^2d\alpha\\
&-(ck_1-\frac{1}{2}ck_2|\varepsilon|)\int_\Omega|\bigtriangledown\tilde{w}|^2d\alpha\\
&+\gamma\left(\|\tilde{w}_t\|_{L^2}+c\sqrt{C}\|\bigtriangledown\tilde{w}\|_{L^2}\right),
\end{aligned}
\tag{37}
$$

where the Friedrichs' inequality is used in the first inequality. For any ε satisfying

$$
|\varepsilon|<\min\left\{\frac{2(k_2-cC)}{k_2(2-c)},\ \frac{2k_1}{k_2}\right\}=\varepsilon^*,
\tag{38}
$$

with positive constant c satisfying

$$
0<c<\min\left\{\frac{1}{C},\frac{k_1}{|C-k_2|},2,\frac{k_2}{C}\right\},
\tag{39}
$$

we have

$$
\dot{V}\le-\frac{a_2}{2}\|\tilde{w}\|_2^2+\gamma b\|\tilde{w}\|_2\le-\frac{a_2}{2m_2}V+\frac{b\gamma}{\sqrt{m_1}}\sqrt{V},
\tag{40}
$$

where b is defined in (23) and

$$
\begin{aligned}
&a_2(\varepsilon)\\
&=\min\left\{\frac{k_2}{C}-c-\left(\frac{k_2}{C}+\frac{1}{2}ck_2\right)|\varepsilon|,\ ck_1-\frac{1}{2}ck_2|\varepsilon|\right\}.
\end{aligned}
\tag{41}
$$

Thus, similarly as the proof for Theorem 1, for $W=\sqrt{V}$, we have

$$
\dot{W}\le-\frac{a_2}{4m_2}W+\frac{b\gamma}{2\sqrt{m_1}},
\tag{42}
$$

and then,

$$
\begin{aligned}
W(t)\le&\frac{4b\gamma m_2}{2a_2\sqrt{m_1}}\\
&+\exp\left(-\frac{a_2}{4m_2}t\right)\left(W(0)-\frac{4b\gamma m_2}{2a_2\sqrt{m_1}}\right).
\end{aligned}
\tag{43}
$$

Thus, (36) is derived with the choices of

$$
C_3=\frac{4b\gamma m_2}{2a_2m_1}\sqrt{m_4},\quad \omega_2=\frac{a_2}{4m_2},
\tag{44}
$$

which completes the proof. □

It can be seen from (41) and (43) that as the velocity bias $|\varepsilon|$ increases, the decay rate of the error system would decrease. Although the inaccuracy of the velocity would slow down the convergence of the system, the equation (38) gives a certain range of the velocity bias, which guarantees the converge rate is always larger than zero. The range depends on cC, where the constant $C\ge1$ is estimated from the Friedrichs' inequality, and the choice of c follows from (22). Thus, as long as the bias, if there is any, is limited within this range, our method proposed in this paper can achieve formation tracking control.

5. FORMATION TRACKING CONTROL IN THE 3-D SPACE

It is worth emphasizing that this result is general for formation tracking control in any n-dimensional state space and any m-dimensional topology space. In other words, the proposed formation tracking control framework can be applied to high dimensional spaces together with diversified communication topologies. In this section, several simulation examples are presented for the formation tracking control of MAS with a 2-D topology in the 3-D space, more specifically, on a spherical surface.

5.1. The model under spherical coordinates

Consider the PDE system (3)-(5) with the controller (7) in the 3-D state space under the spherical coordinates (r,θ,ϕ), where the radius is constant: $r=1$, the polar angle $\theta\in[\theta_1,\theta_2]$ with $0<\theta_1,\theta_2<\pi$, and the azimuthal angle $\phi\in[0,2\pi]$. For the sake of simplicity, the coordinate r is omitted from the context in the sequel.

Denote the state as

$$
\mathbf{w}(\theta,\phi,t):=(x(\theta,\phi,t),y(\theta,\phi,t),z(\theta,\phi,t))^T,
$$

then each of the states $x(\theta,\phi,t)$, $y(\theta,\phi,t)$ and $z(\theta,\phi,t)$ satisfies the following PDE:

$$
\begin{aligned}
w_{tt}(\theta,\phi,t)=&k_1\left(\cot(\theta)w_\theta+w_{\theta\theta}+\frac{w_{\phi\phi}}{\sin^2(\theta)}\right)\\
&-k_1\left(\cot(\theta)w^d_\theta+w^d_{\theta\theta}+\frac{w^d_{\phi\phi}}{\sin^2(\theta)}\right)\\
&+k_2\left(\cot(\theta)w_{t\theta}+w_{t\theta\theta}+\frac{w_{t\phi\phi}}{\sin^2(\theta)}\right),
\end{aligned}
\tag{45}
$$

where $k_2>0$ is the control gain and the Laplacian in spherical coordinates is used. The corresponding boundary conditions and initial conditions are thus

$$
w(\theta_1,\phi,t)=w^d(\theta_1,\phi,t)+f_i(t),
\tag{46}
$$

$$
w(\theta_2,\phi,t)=w^d(\theta_2,\phi,t)+f_i(t),
\tag{47}
$$

$$
w(\theta,\phi,0)=w_0(\theta,\phi),\quad w_t(\theta,\phi,0)=w_1(\theta,\phi),
\tag{48}
$$

where f_i, $i=1,2,3$, denoting the projection of the target orbit along the x, y and z axes, corresponds to the x,y,z-PDEs respectively. Note that with the spherical surface being the topology space, the control algorithm requires only two groups of agents to serve as leader, where the number depends on the way of discretization to ϕ.

The spherical harmonics $\{Y_l^m(\theta,\phi);\ l\in\mathbb{N},m\in\mathbb{Z},|m|\le l\}$ forms an orthogonal basis for $L^2([\theta_1,\theta_2]\times[0,2\pi])$ in the spherical coordinates [26], where

$$
Y_l^m(\theta,\phi)=\sqrt{\frac{2l+1}{4\pi}\frac{(l-m)!}{(l+m)!}}P_l^m(\cos(\theta))\tilde{\mathbf{w}}^{\mathrm{j}m\phi},
$$

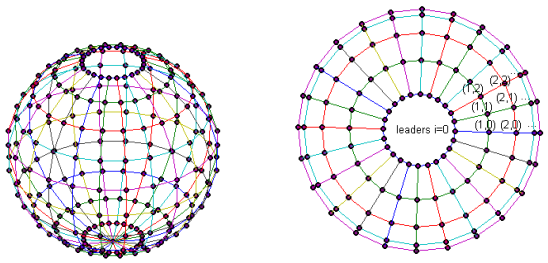

(a) (b)

Fig. 1. Communication topology of the agents. (a) The frontal view. (b) The top view (for half the sphere).

with the associated Legendre polynomial P_l^m defined as

$$P_l^m(s) = \frac{1}{2^l l!}(1-s^2)^{\frac{m}{2}} \frac{\mathrm{d}^{l+m}}{\mathrm{d}s^{l+m}}(s^2-1)^l.$$

Therefore, any desired formation manifold in $L^2([\theta_1,\theta_2]\times[0,2\pi])$ can be represented as follows:

$$w^d(\theta,\phi) = \sum_{l=0}^{\infty}\sum_{m=-l}^{l} w_l^m Y_l^m(\theta,\phi), \tag{49}$$

where

$$w_l^m = \int_0^{2\pi}\int_0^{\pi} w^d(\theta,\phi) Y_l^{m*}(\theta,\phi)\sin(\theta)d\theta d\phi.$$

Here, * denotes the (complex) conjugate operator when Y_l^m is complex harmonics.

5.2. Distributed control law

By discretizing the PDE model (45)–(47), a distributed control algorithm for the agents is obtained. The discretized topology in spherical surface shown in Fig. 1, in which there are $(M+1)\times(N+1)$ agents labeled by identification number $(i,j)\in\{0,..,M\}\times\{0,...,N\}$ corresponding to the location (ih_θ, jh_ϕ) on topology with the polar angle step $h_\theta = \frac{\theta_2-\theta_1}{M}$ and azimuthal angle step $h_\phi = \frac{2\pi}{N}$.

The agents on the boundary are chosen as leaders, labeled by $i=0$ and $i=M$ for all $j=0,1,\cdots,N$ and the other agents are followers. The protocol for the leaders is directly from the boundary condition (46) and (47):

$$x_{0,j}(t) = x^d(\theta_1,\phi)+f_1(t),$$
$$x_{M,j}(t) = x^d(\theta_2,\phi)+f_1(t).$$

Discretizing (45) through finite difference methods in spherical coordinates, we get the following coordinated control protocol for each follower (i,j), $i=1,\cdots,M-1$ and $j=0,\cdots,N-1$:

$$\begin{aligned}\ddot{x}_{i,j}(t) =& k_1\left(\frac{\cot(ih_\theta)}{2h_\theta}(x_{i+1,j}-x_{i-1,j})\right.\\ &\left.+\frac{x_{i+1,j}-2x_{i,j}+x_{i-1,j}}{h_\theta^2}+\frac{x_{i,j+1}-2x_{i,j}+x_{i,j-1}}{h_\phi^2\sin^2(ih_\theta)}\right)\\ &-k_1\left(\frac{\cot(ih_\theta)}{2h_\theta}(x^d_{i+1,j}-x^d_{i-1,j})\right.\\ &\left.+\frac{x^d_{i+1,j}-2x^d_{i,j}+x^d_{i-1,j}}{h_\theta^2}+\frac{x^d_{i,j+1}-2x^d_{i,j}+x^d_{i,j-1}}{h_\phi^2\sin^2(ih_\theta)}\right)\\ &+k_2\left(\frac{\cot(ih_\theta)}{2h_\theta}(\dot{x}_{i+1,j}-\dot{x}_{i-1,j})\right.\\ &\left.+\frac{\dot{x}_{i+1,j}-2\dot{x}_{i,j}+\dot{x}_{i-1,j}}{h_\theta^2}+\frac{\dot{x}_{i,j+1}-2\dot{x}_{i,j}+\dot{x}_{i,j-1}}{h_\phi^2\sin^2(ih_\theta)}\right).\end{aligned}$$

From the above control protocol, the followers only need to use local information from their neighbors. For periodical properties of spherical coordinates, let $x_{i,-1}=x_{i,N}$ or $x_{i,N+1}=x_{i,0}$, respectively. The control protocol along the y and z axes can be written in a similar form, so we omit them.

5.3. Simulations

Consider the PDE system (3)-(5) with $k_1=1.6$, where the controller is designed as (7) with the gain $k_2=0.7$. All simulations are carried on with 41×51 agents, i.e., $M=40$, $N=50$.

First, four examples of the desired formation with x,y,z all governed by (49) are shown in Fig 2. In these numerical examples, we let $\theta_1=0.01$ and $\theta_2=\pi-0.01$. In particular, the manifolds are described by (a) sphere $x^d=\sin(\phi)\cos(\theta)$, $y^d=\sin(\phi)\sin(\theta)$ and $z^d=\cos(\phi)$; (b) spherical harmonics Y_3^2 with functions $x^d=|Y_3^2(\theta,\psi)|^2\sin(\phi)\cos(\theta)$, $y^d=|Y_3^2(\theta,\psi)|^2\sin(\phi)\sin(\theta)$ and $z^d=|Y_3^2(\theta,\psi)|^2\cos(\phi)$; (c) hyperbolic surface $x^d=\cosh(\phi)\cos(\theta)$, $y^d=\cosh(\phi)\sin(\theta)$ and $z^d=1.2\sinh(\phi)$ and (d) spherical harmonics Y_2^2.

Fig. 3 depicts a formation tracking process that the multi-agent system track the target on a circular orbit and at the same time keep the desired formation. The agents begin at initial position $(0,b_0,0)$ with $b_0=0.2$ and in the initial formation Y_2^2 (Fig. 2(f)). After that, the desired formation becomes spherical harmonics Y_3^2. At the same time, the agents in formation are required to move on a target orbit governed by $x=b_0\cos(a_0t)\cos(\psi)$, $y=b_0\cos(a_0t)\sin(\psi)$ and $z=b_0\sin(a_0t)$, where $a_0=1$, $\psi=\pi/9$.

The desired trajectory has a varying velocity which is only known to the leaders, so there exist tracking errors. However, the errors are almost unnoticeable in Fig. 3. The readers could also refer to the simulation video from [27]. The tracking errors versus time are shown in Fig. 4. After the transient evolution is settle down, the tracking errors converges and bounded by the acceleration peak (0.16). The mean of the squared position errors $\tilde{w}(\alpha,t)$ is bounded by a sine-like function, and the velocity errors are much smaller and almost converge to zero.

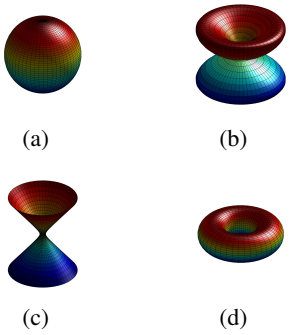

Fig. 2. Agent formation manifolds. (a) Sphere. (b) Spherical harmonics Y_3^2. (c) Hyperbolic surface. (d) Spherical harmonics Y_2^2.

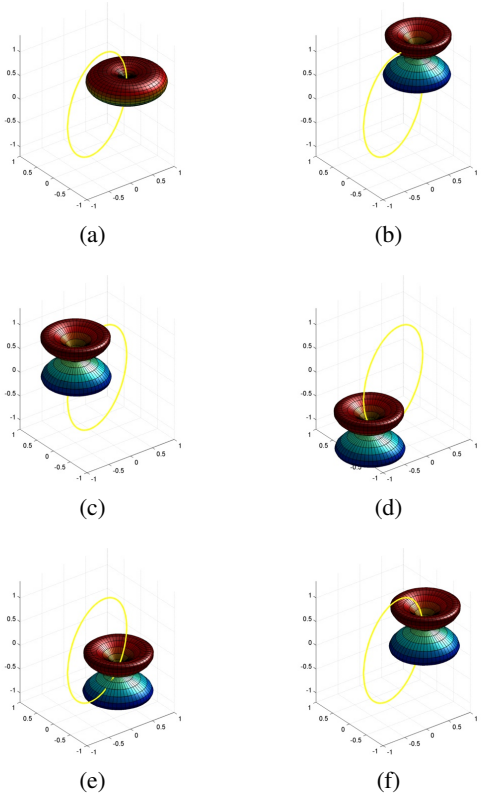

Fig. 3. Formation tracking snapshots. The formation begins with a tire tread pattern (a) $t = 0$. And then the formation transform to Spherical harmonics Y_3^2 and at the same time moving to the top of the target orbit (b) $t = 1.84s$. After that the formation keep unchanged and move on the target circular orbit at $t = 9.84s$ (c), $t = 16.8s$ (d), and $t = 24.4s$ (e). Finally the formation (f) $t = 31.4s$.

Consider the perturbation of the velocity (within a range) through assignment of parameter ε to be a white noise with variance 0.5. It is obvious from Fig. 5 that although the tracking errors with velocity uncertainty converge more slowly and their transient fluctuations are greater than the case without velocity uncertainty, the errors still converge and bounded.

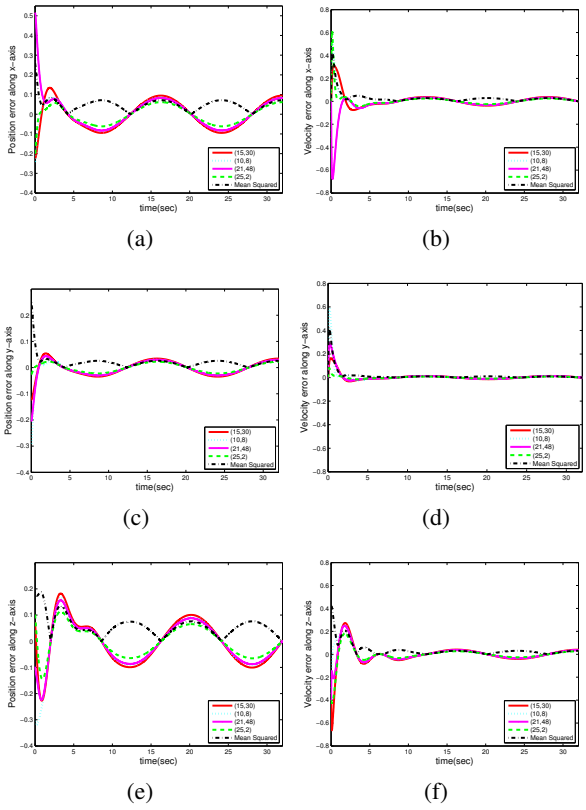

Fig. 4. Position and velocity tracking errors with $\varepsilon = 0$ along the x-axis (a) (b), y-axis (c) (d) and z-axis (e) (f).

In order to check the capability of the system tracking a target with rapid speed, we consider an example that the agents track an orbit on a straight line with a rapid speed. The target orbit is $\mathbf{f}(t) = 2t(1,1,1)^T$, and the desired formation still use Y_3^2. As shown in Figure 6, the tracking errors converge almost to zero within $8s$. Furthermore, it is worth testing the performance of the control algorithm in the case that one or two agents suddenly lose connection with its neighbors when the system is moving along the desired orbit. Fig. 7 (a) and (b) show the simulation results of followers $(20,25)$, $(20,28)$ losing connection with the system at $t = 7.2s$ for 2 seconds. Fig. 7(c) and (d) show another simulation results of leaders $(31,25)$, $(31,42)$ losing connection at $t = 7.2s$ for 2 seconds. Once communication fails, the information from the neighbors that cannot be obtained is replaced by the previous one until the communication is reconnected. The simulation results illustrate that temporal communication failure has little effect on the system by utilizing the proposed control protocol.

For all the above simulations, the computation complexity is $\mathcal{O}((M+1)(N+1)L)$ with L being the number

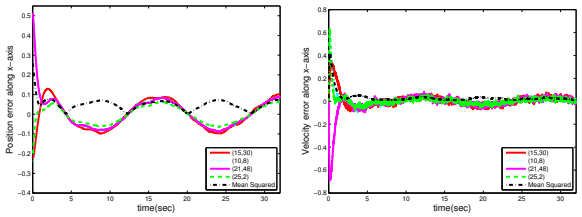

(a) (b)

Fig. 5. Position (a) and velocity (b) tracking errors along x-axis when ε is a white noise with variance 0.5.

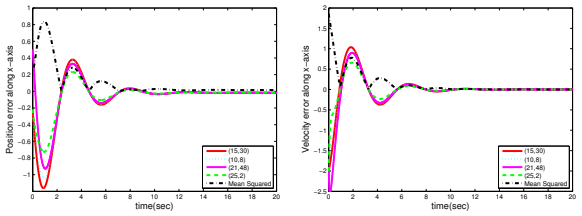

(a) (b)

Fig. 6. Position (a) and velocity (b) tracking errors along x-axis when all the agents move quickly along a straight line.

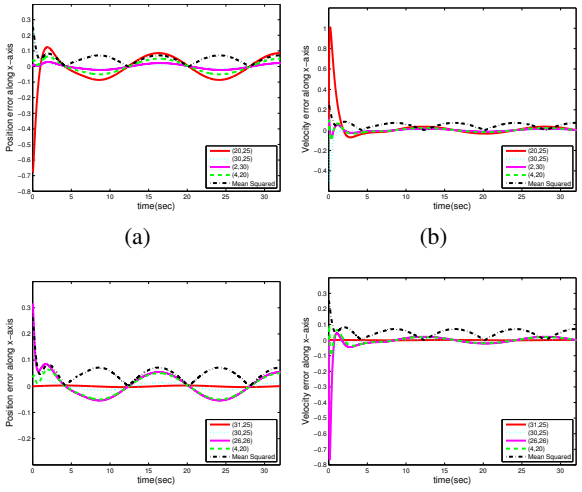

(a) (b)

(c) (d)

Fig. 7. Position (a) and velocity (b) tracking errors along the x-axis with $\varepsilon = 0$ when followers $(20,25)$ and $(20,28)$ lose connection with the system. Position (a) and velocity (b) tracking errors along the x-axis with $\varepsilon = 0$ when leaders $(31,25)$ and $(31,42)$ lose connection.

of iterations [28].

6. CONCLUSION AND FUTURE WORKS

A wave PDE is introduced to model the distributed large-scale MAS. In order for the agents to track some desired formation moving along some desired trajectory, a leader-follower strategy is employed. The desired formation and trajectory are only known by the leaders, while each follower knows only its relative position and velocity with respect to those of its neighbors. A distributed inner controller consisting of a Kelvin-Voigt damping term is then designed, actuating on the followers. The tracking error between the desired and actual positions of the agents is uniformly ultimately bounded by a constant directly proportional to the agent acceleration. Moreover, robustness of the control law to a perturbation in the velocity measurement is also proved.

The extension of this control algorithm to more complicate communication topologies can be considered as a future research topic, and it can possibly be achieved by using different discretization schemes and multi-indices [23, Chapter 3]. It is also worth considering the corresponding problem with the dynamics of non-point agent systems, such as the nonholonomic wheel robots and the rigid body systems. Furthermore, due to the limitation of the physical systems, the amplitude saturation problem [29] of the acceleration actuator can be investigated.

REFERENCES

[1] L. Fang and P. J. Antsaklis. "Decentralized formation tracking of multi-vehicle systems with nonlinear dynamics," *Proc. of the 14th Mediterranean Conf. on Control and Automation, MED'06*, pp. 1-6, 2006.

[2] K. K. Oh, M. C. Park, and H. S. Ahn, "A survey of multi-agent formation control," *Automatica*, vol. 53, pp. 424-440, March 2015. [click]

[3] Y. Cao, W. Yu, W. Ren, and G. Chen, "An overview of recent progress in the study of distributed multi-agent coordination," *IEEE Transactions on Industrial Informatics*, vol. 9, no. 1, pp. 427-438, February 2013. [click]

[4] G. Antonelli, F. Arrichiello, F. Caccavale, and A. Marino, "Decentralized time-varying formation control for multi-robot systems," *The International Journal of Robotics Research*, vol. 33, no. 7, pp. 1029-1043, May 2014.

[5] R. Olfati-Saber, J. A. Fax, and R. M. Murray, "Consensus and cooperation in networked multi-agent systems," *Proc. of the IEEE*, vol. 95, no. 1, pp. 215-233, January 2007. [click]

[6] M. Rubenstein, A. Cornejo, and R. Nagpal, "Programmable self-assembly in a thousand-robot swarm," *Science*, vol. 345, no. 6198, pp. 795-799, August 2014. [click]

[7] F. Y. Hadaegh, S. J. Chung, and H. M. Manohara, "On development of 100-gram-class spacecraft for swarm applications," *IEEE Systems Journal*, vol. 10, no. 2, pp. 673-684, June 2016. [click]

[8] T. Vicsek, A. Zafeiris, "Collective motion". *Physics Reports*, vol. 517, no. 3, pp. 71-140, 2012. [click]

[9] A. Sarlette, and R. Sepulchre, "A PDE viewpoint on basic properties of coordination algorithms with symmetries,"

Proc. of the 48th IEEE Conf. on Decision and Control and 28th Chinese Control Conf., pp. 5139-5144, 2009.

[10] G. Ferrari-Trecate, A. Buffa, and M. Gati, "Analysis of coordination in multi-agent systems through partial difference equations," *IEEE Transactions on Automatic Control*, vol. 51, no. 6, pp. 1058-1063, June 2006. [click]

[11] T. Meurer, and M. Krstic, "Finite-time multi-agent deployment: A nonlinear PDE motion planning approach," *Automatica*, vol. 47, no. 11, pp. 2534-2542, November 2011. [click]

[12] P. Frihauf, and M. Krstic, "Leader-enabled deployment onto planar curves: A PDE-based approach," *IEEE Transactions on Automatic Control*, vol. 56, no. 8, pp. 1791-1806, August 2011. [click]

[13] J. Qi, R. Vazquez, and M. Krstic, "Multi-agent deployment in 3-D via PDE control," *IEEE Transactions on Automatic Control*, vol. 60, no. 4, pp. 891-906, April 2015. [click]

[14] N. Ghods, and M. Krstic, "Multi-agent deployment over a source," *IEEE Transactions on Control Systems Technology*, vol. 20, no. 1, pp. 277-285, January 2012. [click]

[15] H. Hao, P. Barooah, and P. G. Mehta, "Stability margin scaling laws for distributed formation control as a function of network structure," *IEEE Transactions on Automatic Control*, vol. 56, no. 4, pp. 923-929, April 2011. [click]

[16] C. Xu, Y. Dong, Z. Ren, H. Jiang, and X. Yu, "Sensor deployment for pipeline leakage detection via optimal boundary control strategies," *Journal of Industrial and Management Optimization*, vol. 11, no. 1, pp. 199-216, January 2015.

[17] V. D. Blondel, J. M. Hendrickx, and J.N. Tsitsiklis, "Continuous-time average-preserving opinion dynamics with opinion-dependent communications," *SIAM Journal on Control and Optimization*, vol. 48, no. 8, pp. 5214-5240, October 2010.

[18] H. Rastgoftar and S. Jayasuriya, "Evolution of multi-agent systems as continua," *Journal of Dynamic Systems, Measurement, and Control*, vol. 136, no. 4, pp. 041014, April 2014. [click]

[19] Y. Zhao, Z. Duan, G. Wen, and Y. Zhang, "Distributed finite-time tracking control for multi-agent systems: an observer-based approach," *Systems & Control Letters*, vol. 62, no. 1, pp. 22-28, January 2013.

[20] Y. Cao and W. Ren, "Multi-vehicle coordination for double-integrator dynamics under fixed undirected/directed interaction in a sampled-data setting," *International Journal of Robust and Nonlinear Control*, vol. 20, no. 9, pp. 987-1000, May 2010.

[21] J. Qi, F. Pan, and J.-P. Qi, "A PDE approach to formation tracking control for multi-agent systems," *Proc. of the 34th Chinese Control Conference*, pp. 7136-7141, 2015.

[22] X. Dong, B. Yu, Z. Shi, and Y. Zhong, "Time-varying formation control for unmanned aerial vehicles: Theories and applications," *IEEE Transactions on Control Systems Technology*, vol. 23, no. 1, pp. 340-348, January 2015.

[23] T. Meurer, *Control of Higher-dimensional PDEs: Flatness and Backstepping Designs*, Springer Science & Business Media, 2012. [click]

[24] M. Krstic and A. Smyshlyaev, *Boundary Control of PDEs: A Course on Backstepping Designs*, SIAM, 2008.

[25] S. Kawashima, and Y. Shibata, "Global existence and exponential stability of small solutions to nonlinear viscoelasticity," *Communications in Mathematical Physics*, vol. 148, no. 1, pp. 189-208, August 1992.

[26] H. Groemer, *Geometric Applications of Fourier Series and Spherical Harmonics*, Cambridge University Press, 1996. [click]

[27] J, Qi, "Simulation movie of a 3-D formation tracking example 2016," https://www.dropbox.com/s/ipnan4c1b6x478r/formationtrackingwave.mp4?dl=0; or http://pan.baidu.com/s/1bbOrHc

[28] A. R. Mitchell and D. F. Griffiths, *The Finite Difference Method in Partial Differential Equations*, John Wiley, 1980.

[29] N. Sun, Y. Fang, H Chen, and L Biao, "Amplitude-saturated nonlinear output feedback antiswing control for underactuated cranes with double-pendulum cargo dynamics," *IEEE Transactions on Industrial Electronics*, vol. 64, no. 3, pp. 2135-2146, March 2017. [click]

Shu-Xia Tang received her Ph.D. in Mechanical Engineering in 2016 from the Department of Mechanical & Aerospace Engineering, University of California, San Diego, USA. She is currently a postdoctoral research fellow and lecturer at the Department of Applied Mathematics, University of Waterloo, Canada. Her main research interests are control and estimation in distributed parameter systems. Recent research also includes optimal actuator and sensor design problems.

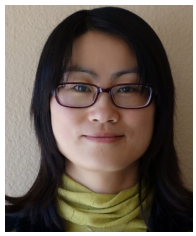

Jie Qi received the Ph.D. degree in Systems Engineering (2005) and the B.S. degree in Automation (2000) from Northeastern University in Shenyang, China. She is currently a Professor in Automation Department, Donghua University, China. Her research interests include multi-agent cooperative control, the control of distributed parameter systems, complex system modeling and intelligent optimization.

Jing Zhang is currently pursuing the Ph.D. degree with the College of Information Science and Technology, Donghua University, Shanghai, China. She received the M.S. degree in Control Science and Engineering (2017) from Donghua University and the B.S. degree in Automation (2013) from Shanxi University, Taiyuan, China. Her research interests include boundary control and multi-agent cooperative control.